HHS Public Access

Author manuscript

Science. Author manuscript; available in PMC 2016 December 24.

Published in final edited form as:

Science. 2016 June 24; 352(6293): 1581–1586. doi:10.1126/science.aaf3892.

Tissue adaptation of regulatory and intraepithelial CD4+ T cells controls gut inflammation

Tomohisa Sujino[1], **Mariya London**[1], **David P. Hoytema van Konijnenburg**[1,2], **Tomiko Rendon**[1], **Thorsten Buch**[3], **Hernandez M. Silva**[4], **Juan J. Lafaille**[4], **Bernardo S. Reis**[1,*], and **Daniel Mucida**[1,*]

[1]Laboratory of Mucosal Immunology, The Rockefeller University, New York, NY 10065, USA
[2]Laboratory of Translational Immunology, University Medical Center Utrecht, the Netherlands
[3]Institute of Experimental Immunology, University of Zurich, Zurich, Switzerland [4]Skirball Institute, New York University School of Medicine, New York, NY 10016, USA

Abstract

Foxp3$^+$ regulatory T cells in peripheral tissues (pT$_{regs}$) are instrumental in limiting inflammatory responses to non-self antigens. Within the intestine, pT$_{regs}$ are located primarily in the lamina propria, while intraepithelial CD4$^+$ T cells (CD4$_{IELs}$), which also exhibit anti-inflammatory properties and depend on similar environmental cues, reside in the epithelium. Using intravital microscopy, we show distinct cell dynamics of intestinal T$_{regs}$ and CD4$_{IELs}$. Upon migration to the epithelium, T$_{regs}$ lose Foxp3 and convert to CD4$_{IELs}$ in a microbiota-dependent fashion, an effect attributed to the loss of the transcription factor ThPOK. Finally, we demonstrate that pT$_{regs}$ and CD4$_{IELs}$ perform complementary roles in the regulation of intestinal inflammation. These results reveal intra-tissue specialization of anti-inflammatory T cells shaped by discrete niches of the intestine.

The gut mucosa is exposed to large amounts of both harmless and potentially pathogenic stimuli on a daily basis, hence diverse immune regulatory mechanisms must operate to avoid inflammatory diseases (1). Peripheral Foxp3-expressing regulatory T cells (pT$_{regs}$) mediate suppression of a variety of immune cells and actively prevent inflammatory bowel diseases and food allergies (2–7). Similar to pT$_{regs}$, Foxp3$^-$CD8αα$^+$CD4$^+$ intraepithelial lymphocytes (CD4$_{IELs}$) depend on retinoic acid (RA) and transforming growth factor (TGF)-β signaling for their development and also have anti-inflammatory properties (4, 8–13). However, while CD4$_{IELs}$ accumulate in the intestinal epithelium, very few total T$_{regs}$ (including pT$_{regs}$ or thymically-derived T$_{regs}$) can be found at this site (fig. S1A and B). We asked whether and how the intestinal environment segregates pT$_{regs}$ and CD4$_{IELs}$, the

*Address correspondence to: B.S.R. (breis@rockefeller.edu) or D.M. (mucida@rockefeller.edu)., Laboratory of Mucosal Immunology, The Rockefeller University, New York, NY 10065, USA.

Supplementary Materials:
Materials and Methods
Figures S1–S4
Movies S1–S3
Reference (35)

transcriptional control involved in this regulation and how this balance affects gut inflammation.

We used intravital multi-photon microscopy (IVM) to investigate whether T_{regs} are actively excluded from the gut epithelium. For tracking in vivo T_{reg} dynamics, we utilized tamoxifen-inducible *Foxp3*$^{CreER\text{-}eGFP}$:*Rosa26*$^{lsl\text{-}tdTomato}$ (i*Foxp3*^{Tomato}) mice (14), which allow T_{reg} fate mapping and the distinction between cells that currently express and cells that once expressed Foxp3. We compared T_{reg} movement patterns in these mice shortly (24 hours) after tamoxifen administration, allowing the visualization of bona fide Tregs (Tomato$^+$), to thymus-derived γδ IEL cell movement patterns (15). We found that more than 80% of TCRγδ^{GFP} cells preferentially remained in the epithelium, while 68% and 14% of Tomato$^+$ cells were considered lamina propria and IE residents, respectively, throughout the duration of multiple independent image recordings (Fig. 1A, B and movies S1 and 2). Among the remaining (~18%) migrating Tomato$^+$ cells, cell tracking indicated that cells moved into the epithelial layer from the lamina propria more frequently than vice-versa (Fig. 1B, C and movie S2). Because ex vivo analysis of the intestinal epithelium revealed a low frequency of Foxp3$^+$ T_{regs} (fig. S1A), these IVM results suggested either preferential cell-death of T_{regs} or T_{reg} conversion into another T cell subtype in this layer.

While all T_{regs} express the CD4-lineage transcription factor ThPOK, or Zbtb7b, CD8αα$^+$CD4$^+$ and more than 50% of Foxp3$^-$CD8α$^-$ CD4$^+$ cells in the small intestine epithelium lack ThPOK expression (fig. S1C). We thus asked whether down-modulation of ThPOK during $CD4_{IEL}$ differentiation influences CD4$^+$ T cell dynamics. We performed IVM using an ovalbumin (OVA)-specific T cell receptor (TCR) transgenic system (OT-II), in which oral OVA exposure leads to incremental ThPOK loss by intestinal CD4$^+$ T cells (10, 16). To allow for the continuous visualization of T cells upon ThPOK loss, we crossed OT-II (*Rag1*$^{-/-}$) with *Thpok*^{GFP} knockin reporter and ubiquitous mRFP1 mice. Sorted naïve (RFP$^+$GFP$^+$) CD4$^+$ T cells from OT-II (RFP *Thpok*^{GFP}) mice were transferred to *Rag1*$^{-/-}$ mice, and recipient mice were kept on an OVA-containing diet for one week and then analyzed by IVM. Computational tracking revealed that roughly 60% of the transferred cells that downregulated ThPOK (RFP$^+$GFP$^-$), and only 20% of ThPOK^{high} cells (RFP$^+$GFP$^+$) remained in the epithelial layer (Fig. 1D, E and movie S3). Migrating ThPOK^{high} cells showed similar movement patterns to T_{reg} cells, with preferential displacement from the lamina propria towards the epithelial layer, suggesting that part of these cells convert into ThPOK^{low} cells, or die, in that compartment (Fig. 1F). These observations indicate that loss of ThPOK corresponds to an IEL-like behavior in CD4$^+$ T cells. Additionally, the discrepancy between the capacity of T_{regs} to visit the intestinal epithelium and their low frequency suggests that this environment may favour T_{reg} plasticity.

To directly address T_{reg} plasticity in the gut tissue, we performed T_{reg} fate mapping using naïve adult *Foxp3*$^{Cre\text{-}YFP}$:*Rosa26*$^{lsl\text{-}DsRed}$ (*Foxp3*^{DsRed}) mice (17). Analysis of peripheral lymphoid tissues isolated from *Foxp3*^{DsRed} mice revealed an almost complete concurrence between Foxp3 reporter (YFP) and DsRed expression, confirming previously the described stability of the T_{reg} lineage (14, 18). However, over 40% of DsRed$^+$ CD4$^+$ T cells in the small intestine epithelium did not express Foxp3 (YFP$^-$), indicating that a considerable number of T_{regs}, or cells that had once turned on the *Foxp3* promoter, lost Foxp3 expression

(fig. S2A). Because previous studies have demonstrated that the majority of “ex-Foxp3” cells in the steady state were derived from uncommitted precursors that transiently upregulated Foxp3 (18), we also performed fate mapping after pulse-labeling i*Foxp3*^{Tomato} mice with tamoxifen (14), a strategy more likely to target bona fide T_{regs} (19). Nevertheless, while stable Foxp3 expression was again observed in several peripheral tissues examined, over 50% of Tomato$^+$ CD4$^+$ T cells that accumulated in the small intestine and almost 10% in the large intestine epithelium isolated from i*Foxp3*^{Tomato} mice no longer expressed Foxp3 fives weeks post tamoxifen administration (fig. S2B and C). The contribution of Tomato$^+$ cells to the CD8αα$^+$ and CD8αβ$^+$ $CD4_{IEL}$ pools was roughly 10% and 25%, respectively (fig. S2D). Consistent with a ThPOK-dependent process, ex-T_{regs} that underwent IEL differentiation showed low levels of ThPOK (fig. S2E). These results indicate that a substantial proportion of intestinal T_{regs} physiologically convert to $CD4_{IELs}$.

Commensal bacteria play a major role in the induction of lamina propria pT_{regs} in the large intestine (3, 5–7, 20). In contrast, we observed an increased frequency of pT_{regs} (Neuropilin-1$^-$ Foxp3$^+$) in the small intestinal epithelium isolated from germ-free (GF) mice when compared to specific pathogen-free (SPF) controls (Fig. 2A). The total T_{reg} number in the epithelial compartment was comparable between GF and SPF mice, even though GF mice showed an almost tenfold reduction in the number of intraepithelial CD4$^+$ T cells (Fig. 2A). Consistent with a reciprocal ThPOK or Foxp3 expression and $CD4_{IEL}$ differentiation, we found an increased frequency of ThPOK^{high} CD4$^+$ T cells and significantly reduced $CD4_{IELs}$ in GF mice (Fig. 2B). We therefore reasoned that the instability of T_{regs} in the gut epithelium was influenced by the microbiota. To address this possibility, we treated i*Foxp3*^{Tomato} mice with broad-spectrum antibiotics for five weeks, starting immediately after tamoxifen exposure. We observed that microbiota depletion completely prevented Foxp3 loss within the Tomato$^+$ CD4$^+$ T cell population, resulting in an accumulation of T_{regs} in the epithelial compartment (Fig. 2C, D). The direct contribution of microbial metabolites versus microbial or dietary antigens to the differentiation of $CD4_{IELs}$ or pT_{regs} occupying the small intestinal epithelium (21) remains to be fully determined. Nevertheless, provision of a TCR ligand can overcome the strict microbiota requirement for $CD4_{IEL}$ differentiation, as demonstrated by the relatively normal $CD4_{IEL}$ differentiation in antibiotic-treated OT-II *Thpok*^{GFP} *Rag1*$^{-/-}$ mice exposed to oral OVA (fig. S2F). Along with the above data, these observations substantiate a microbial-induced plasticity of T_{reg} cells in the epithelium, corroborating intra-tissue specialization and conversion of gut CD4$^+$ T cells.

Next, we interrogated whether the reciprocal properties of pT_{regs} and $CD4_{IELs}$ were influenced by lineage-defining transcription factors. We first determined the role of ThPOK by crossing mice in which exons 2 and 3 of *Thpok* are flanked by *loxP* sites (*Thpok*$^{fl/fl}$)(22) with *Cd4*^{CreER} mice (fig. S3A)(23). *In vivo* administration of tamoxifen to i*Cd4*(Δ*Thpok*) mice (16) one week prior to analysis resulted in a 32% to 48% reduction in the frequency of Foxp3$^+$ T_{regs} in lymphoid and intestinal tissues, respectively, whereas an increase in $CD4_{IELs}$ was observed only in intestinal tissues (Fig. 3A, B). To examine the T_{reg} cell-intrinsic nature of these findings, we next crossed *Thpok*$^{fl/fl}$ with *Foxp3*$^{CreER\text{-}eGFP}$ (fig. S3B) (16). Ex vivo analysis of T cells from i*Foxp3*(Δ*Thpok*) mice one week after tamoxifen treatment did not show a significant decrease in Foxp3 levels in the tissues examined, suggesting that ThPOK was not required for short term stability of the lineage. However,

analysis of T cells from i*Foxp3*(Δ*Thpok*) mice five weeks post-tamoxifen pulse revealed a significant reduction in the frequency and levels of Foxp3 in $CD4^+$ T cells located in most compartments analyzed, with the exception of the large intestine (Fig. 3C, D). Reciprocally, we found an accumulation of $CD8\alpha\alpha^+$ $CD4^+$ T cells in the small intestine (Fig. 3C, D). These data provides further support for a ThPOK role in the regulation of the T_{reg} de novo conversion and stability.

To target the $CD4_{IEL}$ lineage defining transcription factors, we generated mice with conditional deletion of *Runx3* or *Tbx21* (encoding T-bet), which mediate downregulation of ThPOK in developing $CD4_{IELs}$ (9, 10). We analyzed the epithelial compartment of *Cd4*(Δ*Runx3*) mice, and found a reduction in the frequency and in the number of $CD4_{IELs}$ and, conversely, enrichment in T_{regs} (Fig. 3E). Next, we analyzed mice in which *Tbx21* was excised early (driven by $Ox40^{Cre}$ (24)), or late (driven by $E8_{ICre}$ (25)) during the $CD4_{IEL}$ differentiation (16). *Ox40*(Δ*Tbx21*) mice also showed reduced $CD4_{IEL}$ and roughly a two-fold increase in T_{regs} in the epithelium, while $E8_I$(Δ*Tbx21*) mice showed reduced $CD4_{IELs}$, but normal numbers of T_{regs} in the epithelium when compared to Cre^- control mice (Fig. 3E). Collectively, the above data provide a possible mechanism for the reduced number of T_{regs} in the gut epithelium, where collaboration between Runx3 and T-bet results in downmodulation of ThPOK, and Foxp3, in $CD4^+$ T cells (9, 10).

Oral exposure to TCR ligands results in both pT_{reg} and $CD4_{IEL}$ differentiation in a TGF-β-dependent manner (4, 8, 10, 11, 13, 26). We asked whether the intra-tissue adaptation of pT_{regs} and $CD4_{IELs}$ influences the outcome of T cell responses to dietary antigens by employing a transcription factor-based targeting of these lineages in OVA-specific TCR transgenic mice on $Rag1^{-/-}$ background (16). Conditionally targeting *Runx3* in the OT-II model (OT-II(Δ*Runx3*)) prevented ThPOK loss and $CD4_{IEL}$ differentiation, and also impacted pT_{reg} differentiation in the large intestine while no differences in cytokine production were found when compared to control OT-II mice (fig. S4A–D). Whereas OVA-challenged control OT-II mice showed few or no signs of intestinal inflammation, OT-II(Δ*Runx3*) mice readily developed diarrhea and severe pathology, as confirmed by fecal lipocalin-2 levels (Fig. 4A–C). We concluded that prevention of ThPOK loss and $CD4_{IEL}$ differentiation resulted in a local inflammatory response towards dietary antigens, although the reduction in pT_{regs} could also contribute to the exaggerated inflammatory phenotype observed in the large intestine of OT-II(Δ*Runx3*) mice. In contrast, conditionally targeting *Thpok* by administering tamoxifen to OVA-fed iOT-II(Δ*Thpok*) mice (16) resulted in a severe impairment of pT_{reg} development in all tissues examined with a concomitant increase in $CD4_{IELs}$ in the intestine, while no inflammatory phenotype was observed (fig. S4E–G). We then tested whether the OT-II(Δ*Runx3*) disease phenotype could be rescued, or prevented by wild-type or *Thpok*-deficient OT-II cells (16). We found that transferred wild-type CD45.1 OT-II cells, which could differentiate to both pT_{reg} and $CD4_{IELs}$, as well as $CD4^+$ T cells from tamoxifen-treated iOT-II(Δ*Thpok*) mice, which could only differentiate to $CD4_{IELs}$, rescued the diarrhea and inflammatory phenotype observed in OT-II(Δ*Runx3*) mice (Fig. 4B, C and fig. S4H and I). These data indicate that a balance in ThPOK levels regulates inflammatory, $CD4^+$ T cell-mediated responses to dietary antigens. Additionally, these results suggest that $CD4_{IELs}$ exert a cell-extrinsic control of local intestinal inflammation.

To specifically address the possibility that pT_{regs} and $CD4_{IELs}$ play complementary anti-inflammatory in the intestine, we compared T cell responses to dietary OVA using BALB/c background monoclonal OVA-specific TCR strains, carrying either wild-type Foxp3 or a *scurfy* mutation ($Foxp3^{sf}$)(16), which results in a Foxp3 loss of function (27). In contrast to OT-II mice (C57BL/6 background), TBmc $Foxp3^{wt}$ mice fed an OVA diet showed a high rate of pT_{reg} induction in all tissues examined, but less ThPOK loss and $CD4_{IELs}$ in the epithelium (fig. S4A–C and J–N). Conversely, TBmc $Foxp3^{sf}$ showed a high degree of ThPOK loss and increased $CD4_{IEL}$ development in small intestine, in a frequency that mirrored the relative amounts of pT_{regs} in TBmc $Foxp3^{wt}$ mice (fig. S4J–N). However, no inflammatory phenotype or diarrhea was observed even in the absence of functional Foxp3 in this monoclonal model (Fig. 4D–F). To directly address whether exaggerated $CD4_{IEL}$ differentiation could compensate for the absence of pT_{regs} in TBmc $Foxp3^{sf}$ mice, we depleted $CD4_{IELs}$ using anti-CD8α antibodies during OVA feeding (fig. S4M and N). We found that TBmc $Foxp3^{sf}$ mice treated with anti-CD8α antibodies, but not TBmc $Foxp3^{wt}$ treated with anti-CD8α antibodies or TBmc $Foxp3^{sf}$ treated with control antibodies, showed severe intestinal inflammation and diarrhea (Fig. 4D–F and fig. S4O). These results support a model in which $CD4_{IELs}$ and pT_{regs} cooperate in the regulation of local intestinal inflammation.

The single-layered intestinal epithelium constitutes a uniquely challenging location for immune regulatory processes, given its proximity to highly stimulatory luminal contents and limited spatial organization. It is currently thought that T_{regs} utilize several redundant and complementary mechanisms to suppress inflammatory responses, and their capacity to sense specific environmental cues plays a major role in their function (28–30). The physiological instability that we observe in the T_{reg} lineage within the intestinal epithelium may represent an important modulation of regulatory activity that is coordinated by this particular environment (3, 20, 28, 31, 32). Although our targeting strategies do not discriminate between the function of "ex-T_{regs}" and "directly-converted" $CD4_{IELs}$, natural or forced ThPOK downmodulation was previously associated with an impaired helper function in $CD4^+$ T cells, including reduced production of pro-inflammatory cytokines and reduced expression of costimulatory molecules (8, 10, 33). The data presented here supports a cell-extrinsic suppressive role for $CD4_{IELs}$, although the likely epithelium-specific mechanism employed by these cells to actively regulate or prevent tissue inflammation remains unclear. However, a role for $CD4_{IELs}$ in triggering inflammation via their cytotoxic activity, under specific contexts, is conceivable (8, 34). Nevertheless, the observation that particular environmental cues, such as the microbiota, induce plasticity of seemingly stable lymphocyte lineages may contribute to the understanding of how specialized tissue-adaptation pathways function to balance efficient immune protective responses with tissue tolerance.

Supplementary Material

Refer to Web version on PubMed Central for supplementary material.

Acknowledgments

We are indebted to K. Velinzon and N. Thomas for sorting cells, members of the Nussenzweig lab and The Rockefeller University employees for continuous assistance. We thank S. Hemmers (MSKCC) for generating *Cd4*^{CreER} mice. We especially thank A. Rogoz for outstanding technical support. We thank members of our laboratory, particularly V. Pedicord, and D. Esterhazy, for discussions and critical reading and editing of the manuscript. The data reported in this manuscript are tabulated in the main paper and in the supplementary materials. This work was supported by Leona M. and Harry B. Helmsley Charitable Trust (T.S., D.vK., B.R., D.M.), Japan Foundation for Applied Enzymology and Uehara Memorial Foundation (T.S.), Alexandre Suerman Stipend, Royal Netherlands Academy of Sciences and the Prince Bernhard Cultural Foundation (D.vK.), the Crohn's & Colitis Foundation of America (B.R., D.M.), the Irma T. Hirschl Award (D.M.), a National Institutes of Health NIH R01 DK093674 grant (D.M.). The Rockefeller University Bio-Imaging Resource Center is supported by the Empire State Stem Cell Fund through NYSDOH C023046. D.M. conceived; D.M and B.S.R. supervised this study; T.S., J.J.L., B.S.R. and D.M. designed experiments; T.S., M.L., D.vK., T.R., H.M.S. and B.S.R. performed and analyzed experiments; T.B. provided the *Cd4*^{CreER} strain (23); T.S., M.L., D.vK. and B.S.R. prepared figures and helped with manuscript preparation; D.M. wrote the paper.

References

1. Shale M, Schiering C, Powrie F. CD4(+) T-cell subsets in intestinal inflammation. Immunological reviews. Mar.2013 252:164. [PubMed: 23405904]
2. Bilate AM, Lafaille JJ. Induced CD4+Foxp3+ regulatory T cells in immune tolerance. Annu Rev Immunol. 2012; 30:733. [PubMed: 22224762]
3. Furusawa Y, et al. Commensal microbe-derived butyrate induces the differentiation of colonic regulatory T cells. Nature. Dec 19.2013 504:446. [PubMed: 24226770]
4. Mucida D, et al. Oral tolerance in the absence of naturally occurring Tregs. J Clin Invest. Jul 1.2005 115:1923. [PubMed: 15937545]
5. Smith PM, et al. The microbial metabolites, short-chain fatty acids, regulate colonic Treg cell homeostasis. Science. Aug 2.2013 341:569. [PubMed: 23828891]
6. Arpaia N, et al. Metabolites produced by commensal bacteria promote peripheral regulatory T-cell generation. Nature. Dec 19.2013 504:451. [PubMed: 24226773]
7. Atarashi K, et al. Treg induction by a rationally selected mixture of Clostridia strains from the human microbiota. Nature. Aug 8.2013 500:232. [PubMed: 23842501]
8. Mucida D, et al. Transcriptional reprogramming of mature CD4(+) helper T cells generates distinct MHC class II-restricted cytotoxic T lymphocytes. Nat Immunol. Mar.2013 14:281. [PubMed: 23334788]
9. Reis BS, Hoytema van Konijnenburg DP, Grivennikov SI, Mucida D. Transcription Factor T-bet Regulates Intraepithelial Lymphocyte Functional Maturation. Immunity. Aug 21.2014 41:244. [PubMed: 25148025]
10. Reis BS, Rogoz A, Costa-Pinto FA, Taniuchi I, Mucida D. Mutual expression of the transcription factors Runx3 and ThPOK regulates intestinal CD4(+) T cell immunity. Nat Immunol. Mar.2013 14:271. [PubMed: 23334789]
11. Coombes JL, et al. A functionally specialized population of mucosal CD103+ DCs induces Foxp3+ regulatory T cells via a TGF-beta and retinoic acid-dependent mechanism. J Exp Med. Aug 6.2007 204:1757. [PubMed: 17620361]
12. Hall JA, Grainger JR, Spencer SP, Belkaid Y. The role of retinoic acid in tolerance and immunity. Immunity. Jul 22.2011 35:13. [PubMed: 21777796]
13. Sun CM, et al. Small intestine lamina propria dendritic cells promote de novo generation of Foxp3 T reg cells via retinoic acid. J Exp Med. Aug 6.2007 204:1775. [PubMed: 17620362]
14. Rubtsov YP, et al. Stability of the regulatory T cell lineage in vivo. Science. Sep 24.2010 329:1667. [PubMed: 20929851]
15. Edelblum KL, et al. Dynamic migration of gammadelta intraepithelial lymphocytes requires occludin. Proceedings of the National Academy of Sciences of the United States of America. May 1.2012 109:7097. [PubMed: 22511722]
16. Materials and methods are available as supplementary materials on *Science* Online.

17. Rubtsov YP, et al. Regulatory T cell-derived interleukin-10 limits inflammation at environmental interfaces. Immunity. Apr.2008 28:546. [PubMed: 18387831]
18. Miyao T, et al. Plasticity of Foxp3(+) T cells reflects promiscuous Foxp3 expression in conventional T cells but not reprogramming of regulatory T cells. Immunity. Feb 24.2012 36:262. [PubMed: 22326580]
19. Tanoue T, Atarashi K, Honda K. Development and maintenance of intestinal regulatory T cells. Nat Rev Immunol. May.2016 16:295. [PubMed: 27087661]
20. Atarashi K, et al. Induction of Colonic Regulatory T Cells by Indigenous Clostridium Species. Science. Dec 23.2010
21. Kim KS, et al. Dietary antigens limit mucosal immunity by inducing regulatory T cells in the small intestine. Science. Jan 28.2016
22. Egawa T, Littman DR. ThPOK acts late in specification of the helper T cell lineage and suppresses Runx-mediated commitment to the cytotoxic T cell lineage. Nat Immunol. Oct.2008 9:1131. [PubMed: 18776905]
23. Sledzinska A, et al. TGF-beta signalling is required for CD4(+) T cell homeostasis but dispensable for regulatory T cell function. PLoS biology. Oct.2013 11:e1001674. [PubMed: 24115907]
24. Klinger M, et al. Thymic OX40 expression discriminates cells undergoing strong responses to selection ligands. J Immunol. Apr 15.2009 182:4581. [PubMed: 19342632]
25. Maekawa Y, et al. Notch2 integrates signaling by the transcription factors RBP-J and CREB1 to promote T cell cytotoxicity. Nat Immunol. Oct.2008 9:1140. [PubMed: 18724371]
26. Li MO, Wan YY, Flavell RA. T cell-produced transforming growth factor-beta1 controls T cell tolerance and regulates Th1- and Th17-cell differentiation. Immunity. May.2007 26:579. [PubMed: 17481928]
27. Curotto de Lafaille MA, et al. Adaptive Foxp3+ regulatory T cell-dependent and -independent control of allergic inflammation. Immunity. Jul 18.2008 29:114. [PubMed: 18617425]
28. Josefowicz SZ, Lu LF, Rudensky AY. Regulatory T cells: mechanisms of differentiation and function. Annu Rev Immunol. 2012; 30:531. [PubMed: 22224781]
29. Ohnmacht C, et al. The microbiota regulates type 2 immunity through RORgammat(+) T cells. Science. Aug 28.2015 349:989. [PubMed: 26160380]
30. Sefik E, et al. Individual intestinal symbionts induce a distinct population of RORgamma(+) regulatory T cells. Science. Aug 28.2015 349:993. [PubMed: 26272906]
31. Hooper LV, Macpherson AJ. Immune adaptations that maintain homeostasis with the intestinal microbiota. Nat Rev Immunol. Mar.2010 10:159. [PubMed: 20182457]
32. Bollrath J, Powrie FM. Controlling the frontier: regulatory T-cells and intestinal homeostasis. Seminars in immunology. Nov 30.2013 25:352. [PubMed: 24184013]
33. Vacchio MS, et al. A ThPOK-LRF transcriptional node maintains the integrity and effector potential of post-thymic CD4+ T cells. Nat Immunol. Oct.2014 15:947. [PubMed: 25129370]
34. Jabri B, Abadie V. IL-15 functions as a danger signal to regulate tissue-resident T cells and tissue destruction. Nat Rev Immunol. Dec.2015 15:771. [PubMed: 26567920]
35. Chassaing B, et al. Fecal lipocalin 2, a sensitive and broadly dynamic non-invasive biomarker for intestinal inflammation. PloS one. 2012; 7:e44328. [PubMed: 22957064]

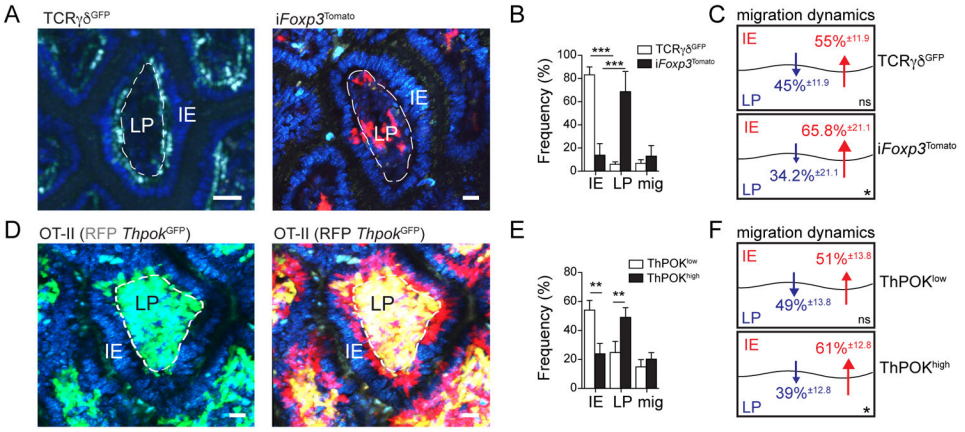

Fig. 1. ThPOK levels correlate with reciprocal T_{reg} and $CD4_{IEL}$ localization and migration dynamics in the intestine

(A to F) Intravital microscopy (IVM) analysis of ileal villi. Mice were injected with Hoechst prior to imaging to visualize all nuclei (blue). Scale bar=10μm. (A) Time-stacked image of TCRγδ^{GFP} (left, green channel) mice and i*Foxp3*^{Tomato} (right, red channel) mice, 24 hours after tamoxifen administration. Images are representative of 20–22 villi from at least 3 independent experiments. (B, C) Frequency of intraepithelial (IE), lamina propria (LP) or migratory TCRγδ^{GFP} and iFoxp3^{Tomato} cells. (C) Percentages within migrating cells. (D to F) Sorted naïve CD4^{+} T cells from OT-II (RFP *Thpok*^{GFP}) mice were transferred to *Rag1*$^{-/-}$ mice and recipient mice were fed an OVA-containing diet for 7 days before IVM analysis. (D) Time-stacked image of GFP^{+} (left, green channel and blue channel overlay) and GFP^{+} (yellow) and GFP^{-} (red) cells (right, green, red and blue channel overlay). Time-stacked images are representative of at least 50 villi from 4 independent experiments. (E) Quantification of tracked GFP^{+} and GFP^{-} cell dynamics from 4 different movies (total 6-paired villi) in 2 independent experiments. (F) Percentages within migrating cells. Cells were tracked using *Imaris* software (Bitplane UK). Data are expressed as mean ± SD from independent movies. ns: not significant, *P<0.05, **P<0.01, ***P<0.001 (Student's t test).

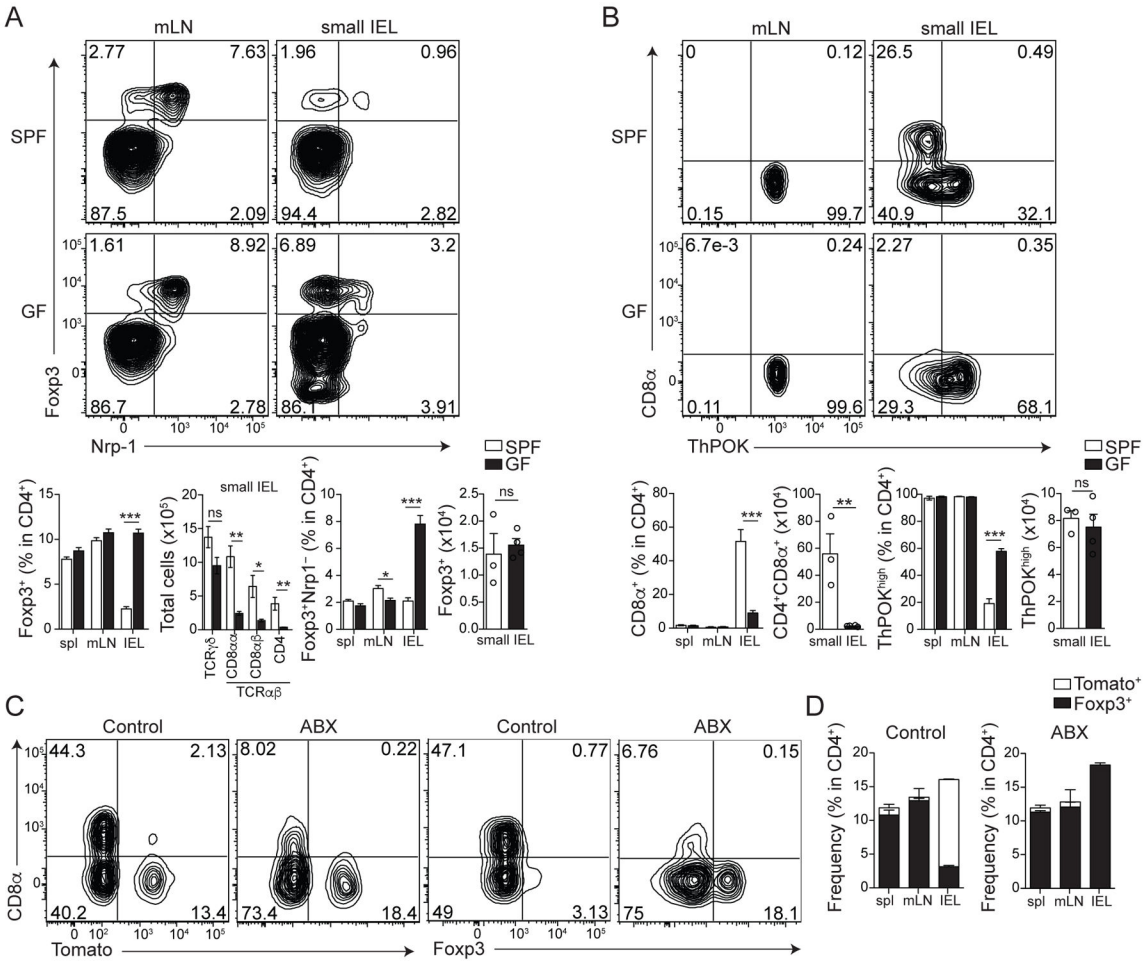

Fig. 2. Microbiota-dependent plasticity of T_{regs} in the intestinal epithelium

(A, B) Flow cytometry analysis of lymphocytes from spleen (spl), mesenteric lymph nodes (mLN) and small intestine epithelium (IEL) of wild-type C57BL/6 mice maintained under specific pathogen-free (SPF) or germ-free (GF) conditions. (A) Surface neuropilin-1 (Nrp-1) and intracellular Foxp3 expression by TCRβ$^+$CD4$^+$CD8β$^-$ cells. Bar graphs represent frequency and total number of Foxp3$^+$ (left) or Foxp3$^+$Nrp-1$^-$ (pTregs) (right) among TCRβ$^+$CD4$^+$CD8β$^-$ cells. Total cell number for T cell populations isolated from the sIELs is also shown. (B) Surface CD8α and intracellular ThPOK expression by TCRβ$^+$CD4$^+$CD8β$^-$ cells. Bar graphs represent frequency and total number of CD8α$^+$ (left) or ThPOK^{high} (right) among TCRβ$^+$CD4$^+$CD8β$^-$ cells. Data expressed as mean ± SD of individual mice (n=6), representative of 3 independent experiments. (C, D) Flow cytometry analysis of lymphocytes from spl, mLN and small intestine IEL of *Foxp3*$^{CreER\text{-}eGFP}$:*Rosa26*$^{lsl\text{-}tdTomato}$ (i*Foxp3*^{Tomato}) mice treated with tamoxifen and maintained with broad spectrum antibiotics for 5 weeks (ABX) or sucralose (CTRL). (C) Surface CD8α and Tomato expression or intracellular Foxp3 among TCRβ$^+$CD4$^+$ cells. (D) Frequency of Foxp3$^+$ (black) and Tomato$^+$ (white) among TCRβ$^+$ CD4$^+$ cells in each tissue. Data expressed as mean ± SD of individual mice (n=3), representative of 3 independent experiments. **P*<0.05, ***P*<0.01, ****P*<0.001 (Student's *t* test).

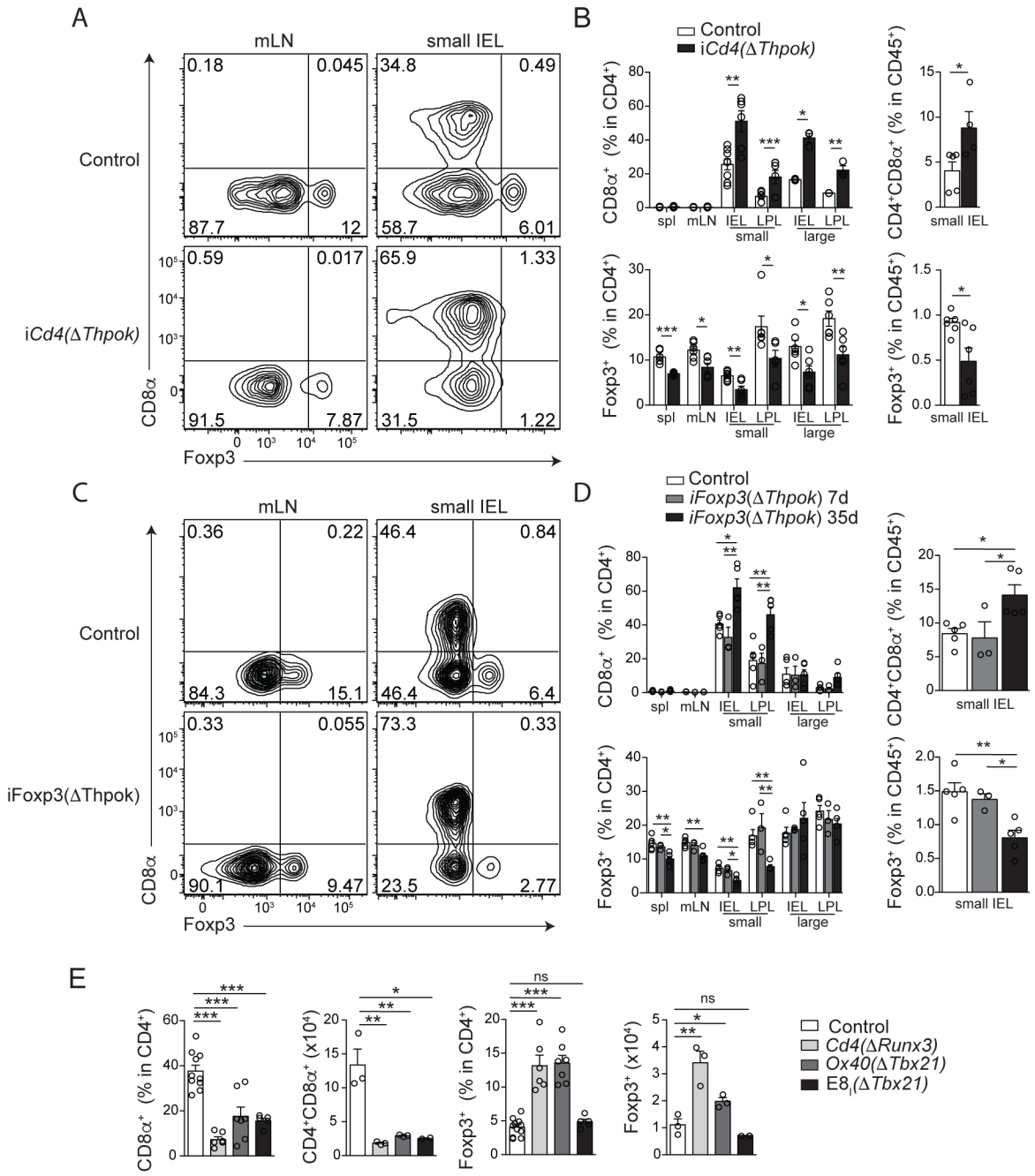

Fig. 3. ThPOK expression by intestinal epithelial CD4$^+$ T cells plays a key role in the reciprocal development of T_{regs} and $CD4_{IELs}$

(A–D) Flow cytometry analysis of lymphocytes from spleen (spl), mesenteric lymph nodes (mLN), small and large intestine epithelium (IEL) and lamina propria (LPL) of inducible conditional *Thpok*-deficient mice. (A, B) *Cd4*^{CreER}:*Thpok*$^{fl/fl}$ (i*Cd4*(Δ*Thpok*)) and (Cre$^-$) *Thpok*$^{f/f}$ littermate control mice 7 days post-tamoxifen administration. (A) Representative contour plot for surface CD8α and intracellular Foxp3 among TCRβ$^+$CD4$^+$CD8β$^-$ cells. (B) Frequency of CD8α$^+$ (upper) and Foxp3$^+$ (lower) among TCRβ$^+$CD4$^+$CD8β$^-$ or among total CD45$^+$ cells in the indicated tissues. Data expressed as means ± SD of individual mice

(n=3–6), representative of 6 independent experiments. (C, D) *Foxp3*^{CreER}:*Thpok*$^{fl/fl}$ (i*Foxp3*(Δ*Thpok*)) and (Cre^{+}) *Thpok*$^{+/+}$ littermate control mice 7 days (shown in D) or 35 days post-tamoxifen administration. (C) Representative contour plot for surface CD8α and intracellular Foxp3 among TCRβ^{+}CD4^{+}CD8β$^{−}$ cells. (D) Frequency of CD8α^{+} (upper) and Foxp3^{+} (lower) among TCRβ^{+}CD4^{+}CD8β$^{−}$ or among total CD45^{+} cells in the indicated tissues. Data expressed as means ± SD of individual mice (n=3–8), representative of 3 independent experiments. (E) Frequency and total number of CD8α^{+} and Foxp3^{+} among TCRβ^{+}CD4^{+}CD8β$^{−}$ cells from sIEL of *Ox40*(Δ*Tbx21*), *Cd4*(Δ*Runx3*), E8$_{I}$(Δ*Tbx21*), and wild-type (WT) mice. Data expressed as mean ± SD of individual mice (n=3–9), representative of 3 independent experiments. **P*<0.05, ***P*<0.01, ****P*<0.001 (Student's *t* test (B), one-way ANOVA with Tukey post-test (D, E)).

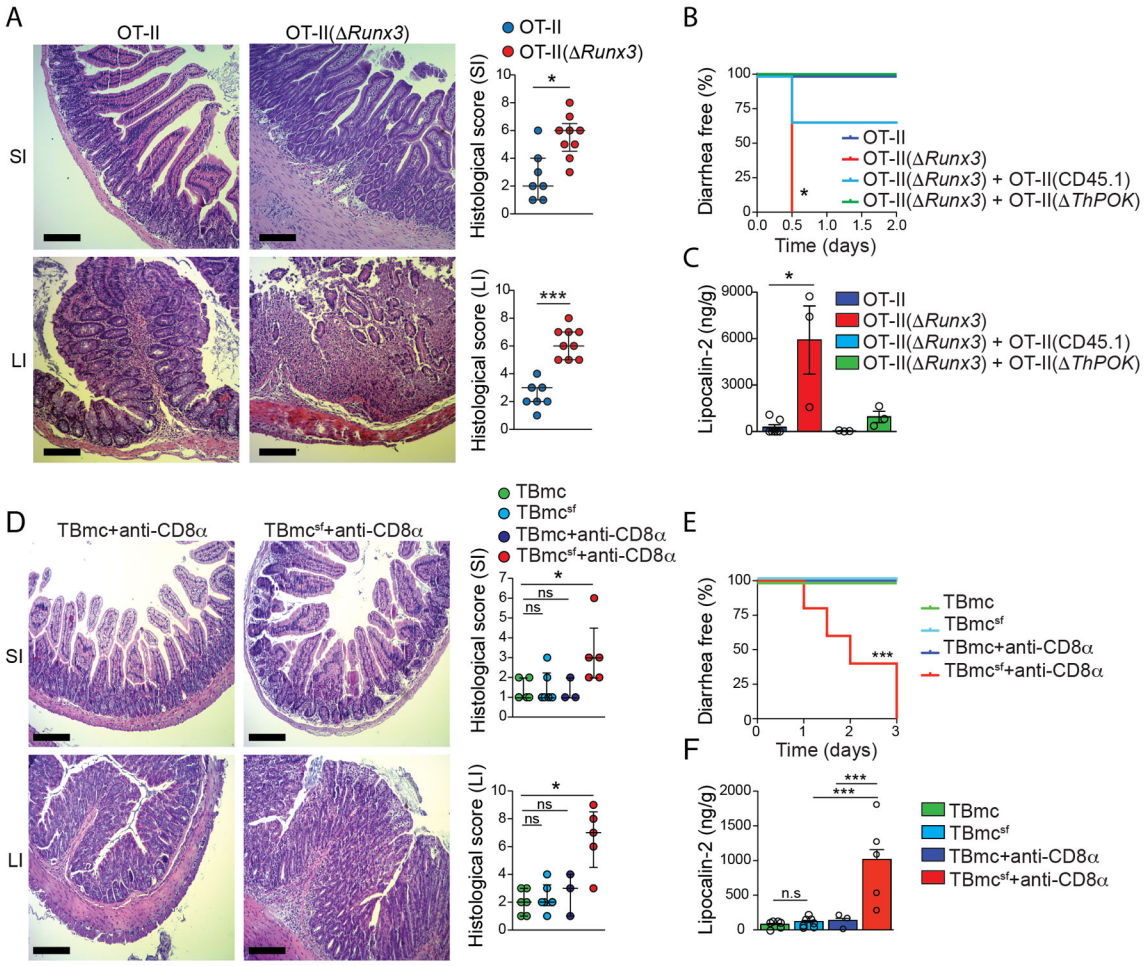

Fig. 4. Complementary roles for pT_{regs} and $CD4_{IELs}$ in regulating local inflammatory response towards dietary antigens

OVA-specific TCR transgenic mice (*Rag1*$^{-/-}$ background) were fed an OVA-containing diet for 7 days. (A–C) *Thpok*^{GFP} OT-II(Δ*Runx3*) and control *Thpok*^{GFP} OT-II mice were analyzed. (A) Hematoxylin and eosin staining of the small intestine jejunum (SI) (upper panels) and the large intestine colon (LI) (lower panels). Original magnification, 40x. Graphs represent histological scores of the SI (upper) and the LI (lower) (each symbol represents one mouse). (B, C) Sorted naïve OVA-specific TCR transgenic cells (TCRVα2^{+}CD4^{+}CD62L^{+}CD44^{low}) from wild-type OT-II or tamoxifen-treated iOT-II(Δ*Thpok*) were transferred to host OT-II(Δ*Runx3*) prior to treatment as in (A). (B) Frequency of diarrhea-free mice after oral OVA challenge. (C) Quantification of fecal Lipocalin-2. (D–F) TBmc Foxp3^{sf} (*scurfy*) and TBmc control treated as in (A), and injected with isotype control or anti-CD8α depleting antibody. (D) Hematoxylin and eosin staining of the SI (upper) and the LI (lower). Original magnification, 40x. Graphs represent histological scores of the SI (upper) and the LI (lower) (each symbol represents one mouse). (E) Frequency of diarrhea-free mice after oral OVA challenge. (F) Quantification of fecal Lipocalin-2. Data expressed as mean +SD or median ± interquartile range (A, D), representative of at least two independent experiments (n=3 to 8 per group). Scale bar, 200

μm. *P<0.05, **P<0.01, ***P<0.001 (Student's t test or Mann-Whitney test (A), one-way ANOVA with Tukey post-test (C, F), Log-rank test (B, E) and Kruskal-Wallis with Dunns post-test (D)).